

## Supplementary Information: Cell-free Extract based Optimization of Biomolecular Circuits with Droplet Microfluidics

Yutaka Hori<sup>a,†</sup>, Chaitanya Kantak<sup>b,†</sup>, Richard M. Murray<sup>a</sup>, Adam R. Abate<sup>b,c,\*</sup>

<sup>a</sup> Department of Computing and Mathematical Sciences, California Institute of Technology, Pasadena, USA.

<sup>b</sup> Department of Bioengineering and Therapeutic Sciences, California Institute for Quantitative Biosciences, University of California, San Francisco, USA. E-mail: adam.abate@ucsf.edu; Fax: +1 415 514 1028; Tel: +1 415 476 9819

<sup>c</sup> Chan Zackerberg Biohub, San Francisco, CA 94158

<sup>†</sup> These authors contributed equally to this work.

\* Corresponding author

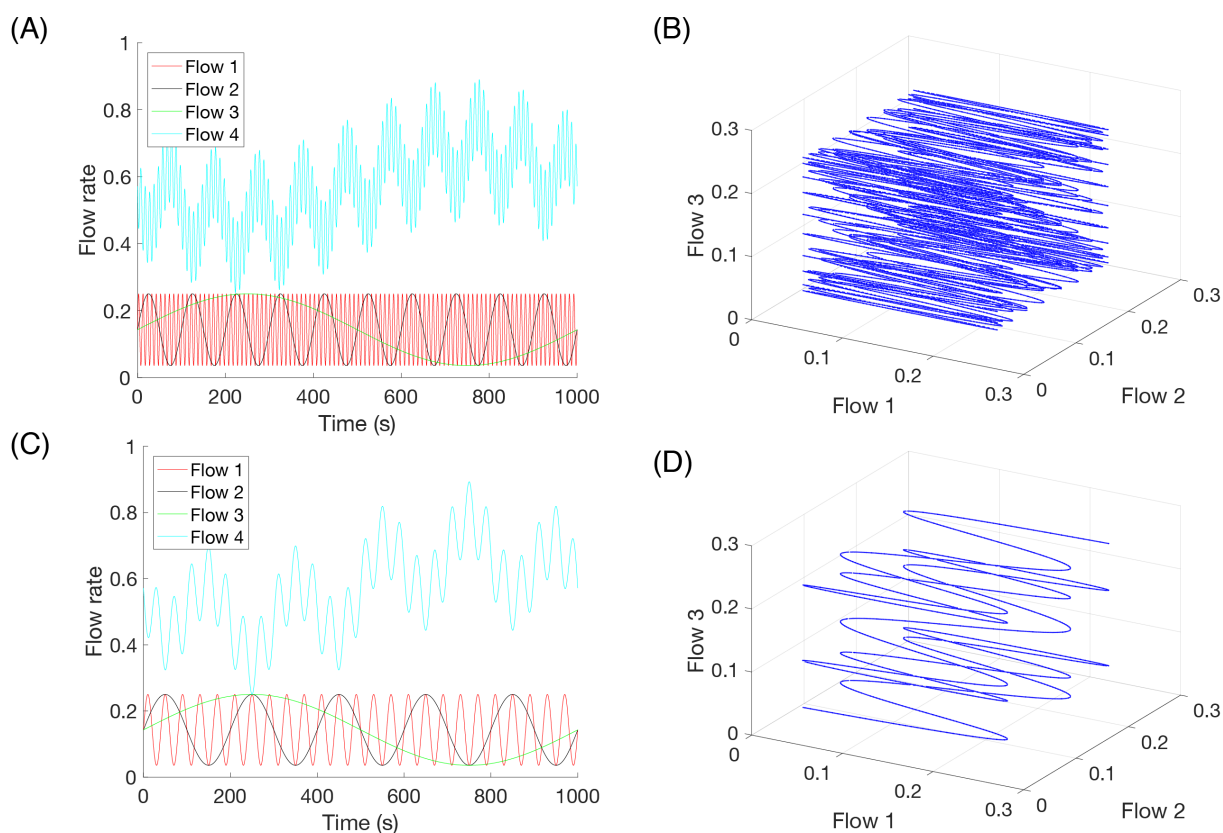


**Figure S1:** *In silico* simulations show that sinusoidal flow rate functions with different periods can efficiently screen the whole parameter space with sufficiently high resolution. (A) The oscillation periods are set as 10, 100 and 1000 seconds for flow 1, 2 and 3, respectively. Flow 4 is a compensation flow to make the sum of the four flow rates to be one. (B) Parameter space screening result using the flow rate functions in (A). (C) The oscillation periods were set as 40, 200 and 1000 seconds for flow 1, 2 and 3, respectively. Flow 4 is a compensation flow to make the sum of the four flow rates to be one. (D) Parameter space screening result using the flow rate functions in (C).

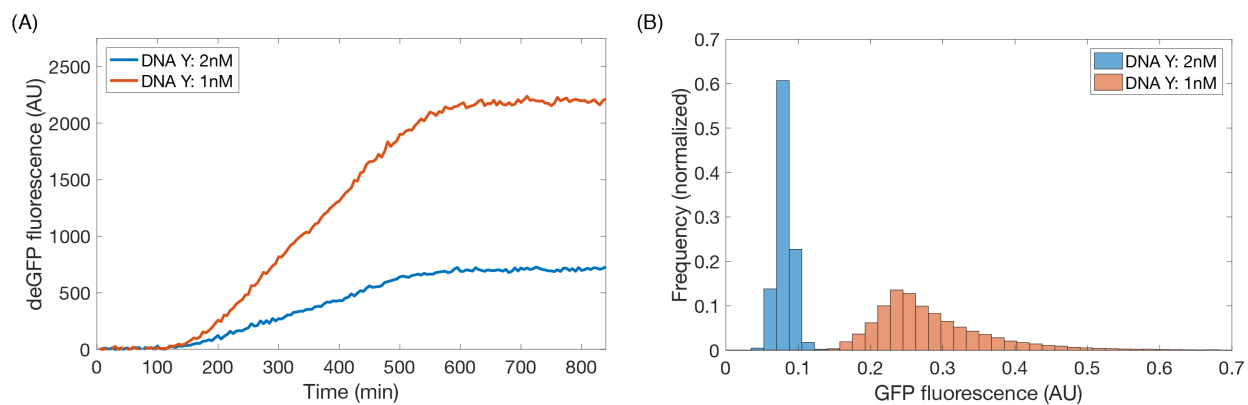


**Figure S2:** (A) Time course of deGFP expression, showing that the cell-free reactions reach steady state at ~10 hr. (B) Distribution of deGFP expression for different concentrations of DNA Y. Expression of deGFP and transcriptional regulation (repression) by TetR are confirmed inside water-in-oil emulsion.

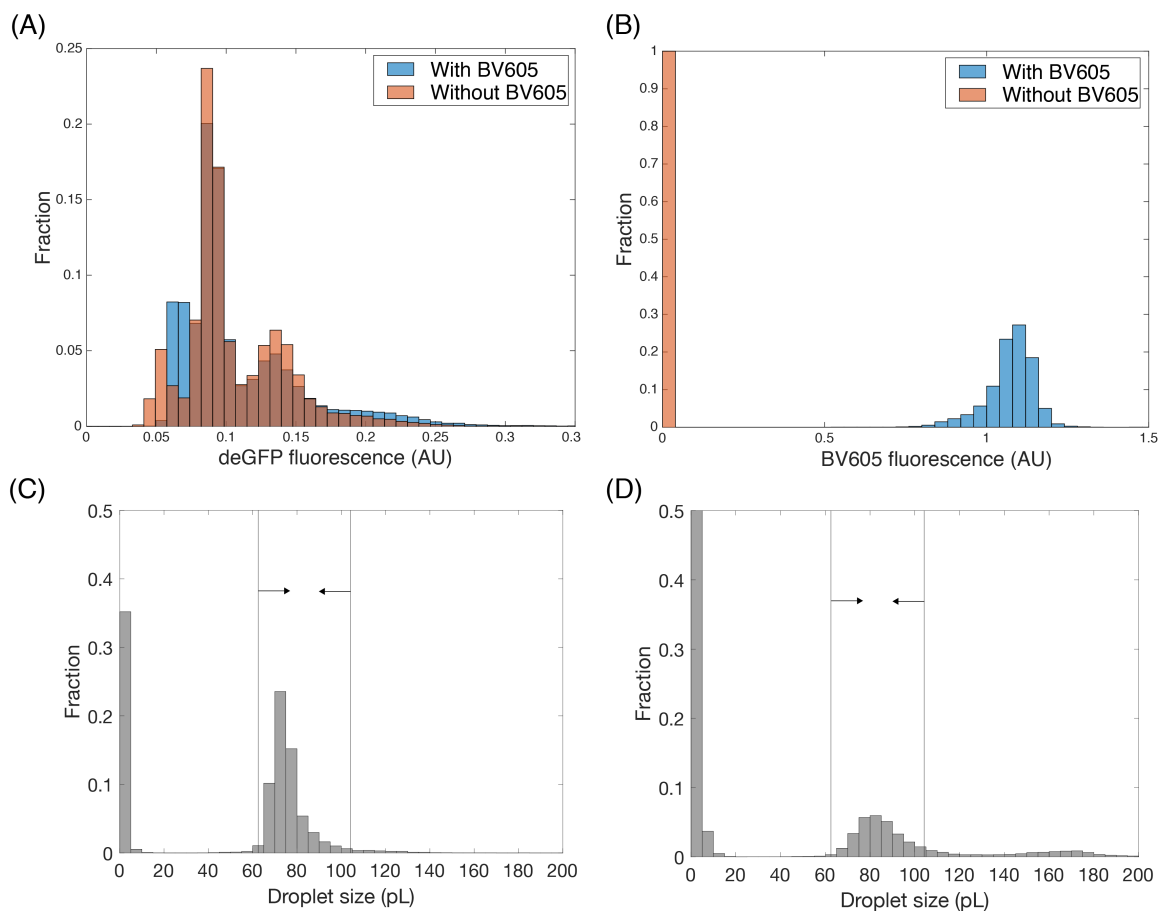


**Figure S3:** The effect of the barcoding dye BV605 on deGFP expression is studied in droplets. Final concentrations in droplets are  $0.30 \mu\text{M}$  of BV605,  $2\text{nM}$  of DNA X,  $4\text{nM}$  of DNA Z and  $0.2\%$  of arabinose. (A) Distribution of deGFP expression in the presence and absence of the dye ( $n=34664$  for droplets with BV605.  $n=18426$  for droplets without BV605). The median of deGFP fluorescence is  $0.0925$  and  $0.0928$  with and without BV605, respectively. The median fluorescence intensities are comparable between the two conditions, implying that the dye BV605 at  $0.30 \mu\text{M}$  does not largely affect the biomolecular reactions. (B) BV605 fluorescence in the presence and absence of the dye. (C) Distribution of the size of the droplets containing BV605. Small and large droplets are time-gated in the histogram (A). (D) Distribution of the size of the droplets not containing BV605. Small and large droplets are time-gated in the histogram (B).

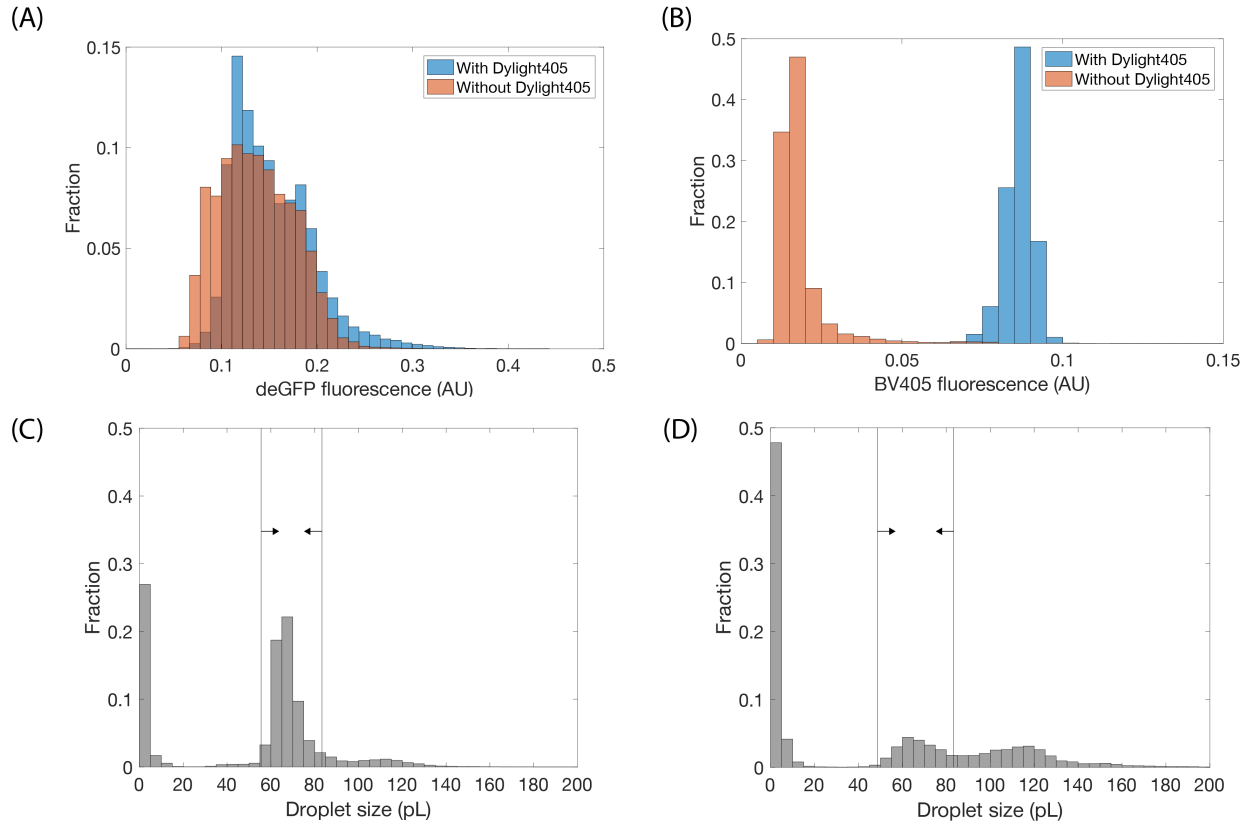


**Figure S4:** The effect of the barcoding dye Dylight405 on deGFP expression is studied in droplets. Final concentrations in droplets are  $0.34 \mu\text{M}$  of Dylight 405,  $2\text{nM}$  of DNA X,  $4\text{nM}$  of DNA Z and  $0.2\%$  of arabinose. (A) Distribution of deGFP expression in the presence and absence of the dye ( $n=108532$  for droplets with Dylight405.  $n=23071$  for droplets without Dylight405). The median of deGFP fluorescence is  $0.145$  and  $0.134$  with and without Dylight405, respectively. The median fluorescence intensities are comparable between the two conditions. (B) Dylight405 fluorescence in the presence and absence of the dye. (C) Distribution of the size of the droplets with Dylight405. Small and large droplets are time-gated in the histogram (A). (D) Distribution of the size of the droplets without Dylight405. Distribution of the size of the droplets not containing Dylight405. Small and large droplets are time-gated in the histogram (B).

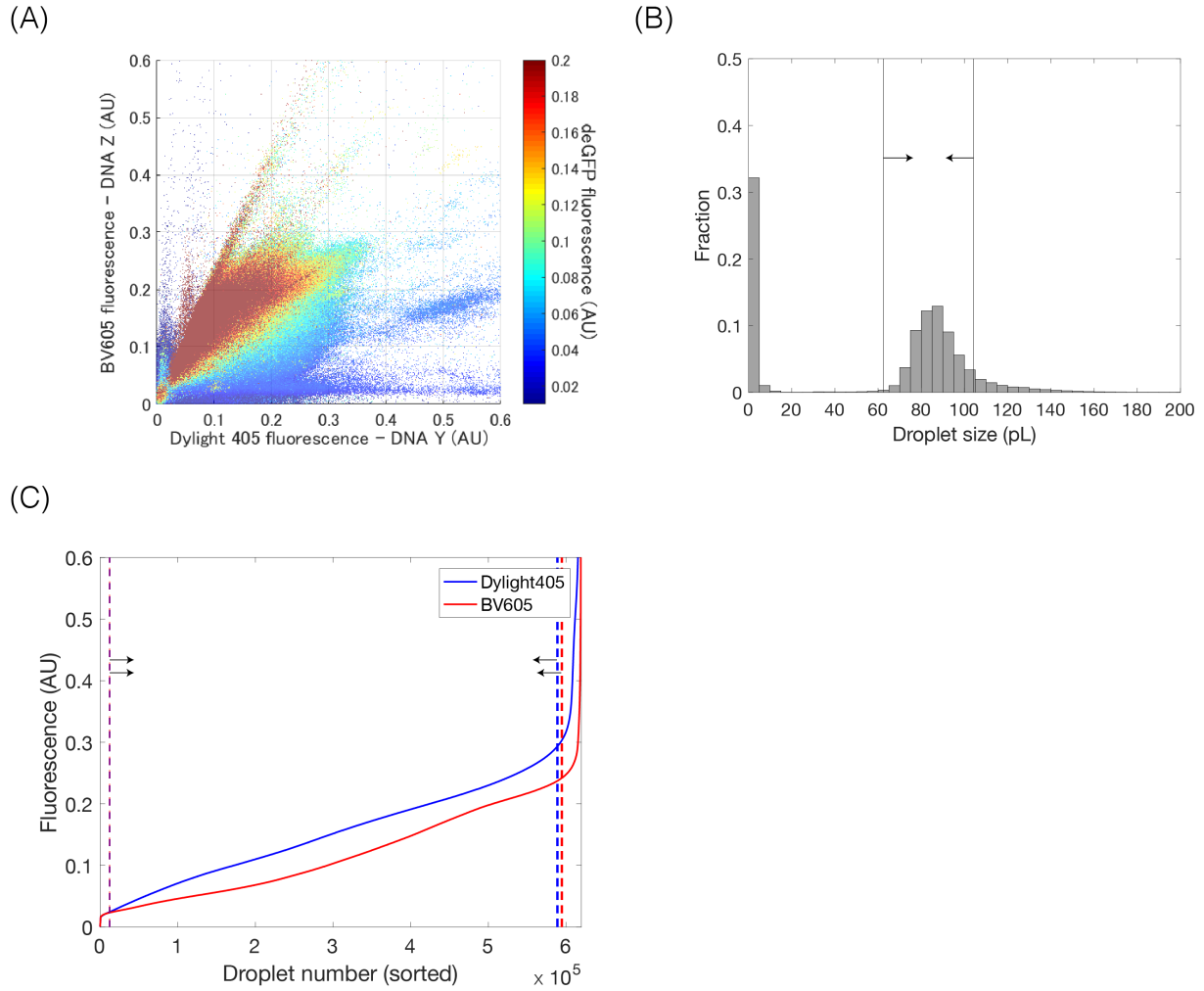


**Figure S5:** (A) Original data for Fig. 3(B) without time-gating ( $n=1044651$ ). (B) Distribution of the droplet size. Small and large droplets outside of the two vertical lines are time-gated. (C) Calibration curve for converting dye fluorescence to plasmid DNA concentrations. Droplets are sorted by fluorescence intensity, and samples outside of the two dotted lines are removed from the analysis as outliers. The dotted lines show the maximum and the minimum fluorescence that corresponds to 4nM and 0.4nM for DNA Y and 0.2nM and 2nM for DNA X. Linear interpolation is used to convert the fluorescence intensity between these two values into plasmid concentrations.

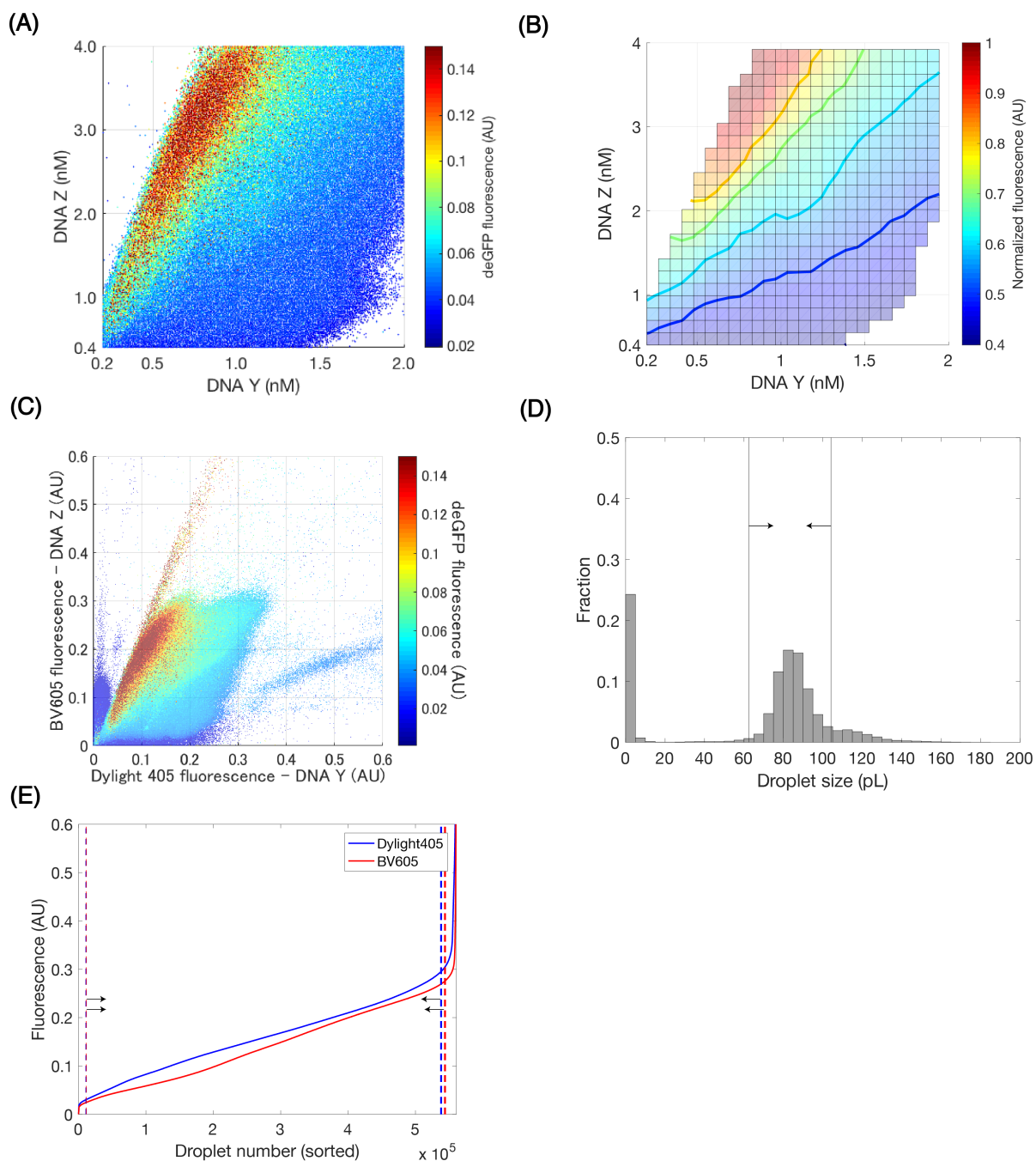


**Figure S6:** The second set of the scanning experiment shows similar trends to the first experiment (Fig. 3). (A) Result of parameter space exploration showing the output of the IFFL biocircuit (deGFP) in terms of DNA Y and DNA Z concentrations ( $n= 558,648$ ). (B) Contour lines of normalized deGFP fluorescence across DNA concentrations. (C) Original data of Fig. S6(A) without time-gating ( $n= 865,496$ ). (D) Distribution of the droplet size. Small and large droplets outside of the two vertical lines are time-gated. (E) Calibration curve for converting dye fluorescence to plasmid DNA concentrations. Droplets are sorted by fluorescence intensity, and samples outside of the two dotted lines are removed from the analysis as outliers. The dotted lines show the maximum and the minimum fluorescence that corresponds to 4nM and 0.4nM for DNA Y and 0.2nM and 2nM for DNA X. Linear interpolation is used to convert the fluorescence intensity between these two values into plasmid concentrations.

## Calculation of droplet volumes

We use the following formula to calculate approximate volumes of droplets based on the duration time of droplet detection.

$$(\text{Droplet volume}) = W \times H \times V \times T,$$

where  $W$  and  $H$  are the width and the height of microfluidic channel, respectively, and  $V$  is the velocity of flow.  $T$  is the time duration of measurement. We used  $W = 60 \mu\text{m}$ ,  $H = 35 \mu\text{m}$  and  $V = 6.61 \mu\text{m/ms}$ , which is equivalent to  $50 \mu\text{L/hr}$ .

The diameter of spherical droplet is expected to be around  $55\mu\text{m}$ , which corresponds to  $87\text{pL}$ , according to our observation of droplets with microscopy. We filter droplets so that only the droplets that belong to the distribution whose peak is around  $87\text{pL}$  is included for the subsequent analyses.

## Mathematical Model

We develop a simple ordinary differential equation (ODE) model of the incoherent feedforward loop circuit based on the law of mass action and the Michaelis-Menten kinetics to predict the qualitative profiles of gene expression using numerical simulations. Let  $(x, y, z)$  denote the concentrations of AraC, TetR and deGFP protein, respectively. We can model the temporal dynamics of these protein concentrations by the following ordinary differential equations (ODEs).

$$\frac{dx(t)}{dt} = -d_1x(t) + c_1u_1$$

$$\frac{dy(t)}{dt} = -d_2y(t) + c_2u_2 \frac{x(t)}{K_1 + x(t)}$$

$$\frac{dz(t)}{dt} = -d_3z(t) + c_3u_3 \frac{x(t)}{(K_1 + x(t))(1 + y(t)/K_2)}$$

where  $d_i$  and  $c_i$  ( $i = 1,2,3$ ) are the degradation and production rates of AraC, TetR and deGFP protein, respectively. Binding of the proteins to the promoter regions is fast compared to degradation and production of these proteins, and thus we assume Michaelis-Menten kinetics and define  $K_i$  ( $i = 1,2$ ) as the Michaelis-Menten constant, at which concentration the promoter is half-maximally expressed. The concentrations of (input) DNA  $X, Y, Z$  are defined as  $u_i$  ( $i = 1,2,3$ ), respectively.

In the numerical simulations, we used the parameter values in the following table.

Table 1. Parameter values used in the numerical simulations

Symbol	Meaning	Value
$d_i$ ( $i = 1,2,3$ )	Degradation rate of proteins	$0.00866 (= \ln(2)/80) \text{ min}^{-1}$ (Half-life: 80 minutes)
$c_1$	Production rate of AraC protein	$40 \text{ nM} \cdot \text{min}^{-1}$
$c_2$	Production rate of TetR protein	$40 \text{ nM} \cdot \text{min}^{-1}$
$c_3$	Production rate of deGFP protein	$12.5 \text{ nM} \cdot \text{min}^{-1}$
$K_1$	Michaelis-Menten constant of pBAD-AraC binding	200 nM
$K_2$	Michaelis-Menten constant of TetO-TetR binding	250 nM